



On Fokker–Planck Equations for Turbulent Reacting Flows. Part 2. Filter Density Function for Large Eddy Simulation

STEFAN HEINZ

*Fachgebiet Strömungsmechanik, Technische Universität München, Boltzmannstr. 15,
D-85747 Garching, Germany; E-mail: heinz@flm.mw.tum.de*

Received 24 January 2003 ; accepted in revised form 19 May 2003

Abstract. The application of large eddy simulation (LES) to turbulent reacting flow calculations is faced with several closure problems. Suitable parametrizations for filtered reaction rates for instance are hardly available in general. A way to overcome these problems is investigated here. This is done by extending LES equations for filtered velocities and scalars (mass fractions of species and temperature) to equations that involve subgrid scale (SGS) fluctuations. Such equations are called filter density function (FDF) methods because they determine the FDF, which is essentially the probability density function of SGS variables. The FDF model considered involves only three parameters: C_0 that controls the generation of velocity fluctuations and two parameters which determine the relaxation of velocity and scalar fluctuations. The consideration of this model may be seen as the analysis of a limiting case: the implications of the most simple equations for the dynamics of SGS fluctuations are investigated in this way. These equations were proved recently by various simulations. Here, the FDF model is used analytically to improve simpler methods. Existing models for the SGS stress tensor in velocity LES equations and the diffusion coefficient in scalar FDF equations are generalized in this way. The advantages of these models compared to existing ones are pointed out. These investigations provide further evidence for the suitability of the FDF model considered and they provide its parameters. A theoretical value $C_0 = 19/12$ is derived, which agrees very well with the results of direct numerical simulation. This estimate implies the same value for the universal Kolmogorov constant of the energy spectrum, which is consistent with the results of many measurements. The other two model parameters can be obtained then by dynamic procedures. Therefore, the closure problems of LES equations are overcome in this way such that adjustable parameters are not involved.

Key words: filter density function, large eddy simulation, stochastic model for subgrid-scale turbulence, subgrid-scale stress tensor, turbulent diffusion coefficient.

1. Introduction

The calculation of turbulent reacting flows by means of direct numerical simulation (DNS) is found to be unfeasible for many relevant flows. The simplest way to overcome this problem is the use of Reynolds-averaged Navier–Stokes (RANS) or probability density function (PDF) equations [14, 33]. The latter methods generalize RANS methods through the incorporation of the dynamics of fluctuations,

which is relevant because it enables the exact treatment of the effects of sources (chemical reaction rates). However, the use of RANS and PDF methods becomes problematic if nonequilibrium flows have to be calculated. That are flows which involve for instance large-scale flow structures or the binary mixing of scalars. To simulate them one has to apply PDF or RANS models that are significantly more complex than simple models applied usually [13]. This leads to a need for the development of alternative methods.

Such an alternative method is given by large eddy simulation (LES). Large-scale processes are resolved without approximations within this approach, which enables predictions that are often found to be more accurate than those of RANS equations [23, 29, 33, 37]. Nevertheless, the use of LES requires the modeling of subgrid scale (SGS) processes. For this reason, the application of LES to reacting flows is faced with the same problem as the use of RANS methods: such LES equations are characterized by the appearance of unknown filtered reaction rates for which accurate parametrizations are unavailable in general. A way to overcome this problem is the use of the PDF methodology to extend LES equations to equations for instantaneous velocities and scalars. This was suggested by Givi [9] and applied first by Madnia and Givi [22]. Pope [31] introduced the concept of a filter density function (FDF) which is essentially the PDF of SGS variables. He showed that the use of this methodology offers for reacting flow simulations the same advantage as the use of PDF methods: chemical reactions appear in a closed form. Gao and O'Brien [5] developed a transport equation for the scalar FDF and offered suggestions for modeling of the unclosed terms in this equation.

One way to use FDF methods is their application to flow simulations. Basically, this was done recently by adopting hybrid FDF methods where the velocity field is calculated by means of conventional LES equations and the scalar transport by a FDF transport equation [2, 15, 34, 45]. Such methods apply algebraic approximations to close the SGS scalar flux in terms of scalar gradients (see the explanations given in the Appendix B). A more general approach consists in the stochastic simulation of both velocity and scalar fields. Such calculations are feasible as shown by Gicquel et al. [8] who performed the first FDF simulations of velocity fields (scalars were not involved). Nevertheless, it turned out that the effort related to the use of velocity-scalar FDF methods is very high. The simulation of velocity fields is six times less expensive than DNS, but it requires 15–30 times more effort than LES methods [8].

Another way to use FDF methods for velocities and scalars is their application to the construction of simpler (hybrid) FDF methods, which are more efficient. This question will be addressed here. First, this is done to improve existing velocity LES and scalar FDF methods by assuring the consistency of these methods. This means for instance that the same model for instantaneous velocities is used to calculate (within the frame of a hybrid method) filtered velocities and the transport of scalars in physical space, or different contributions to algebraic expressions for the SGS stress tensor. The application of such consistent methods was found to be

of remarkable relevance to the use of PDF methods [24, 25, 44], so that the same may be expected with regard to the use of FDF methods. The second reason for performing this analysis is the possibility to assess FDF models for velocities and scalars through the comparison of their implications with well-investigated phenomenological models. This complements their assessment by means of specific flow simulations. It enables more general insight into the suitability of models and the choice of model parameters (e.g., for the case that backscatter effects have to be involved).

The paper is organized as follows. Existing models for velocities and scalars will be combined to a model for the joint velocity-scalar FDF in Section 2. The consideration of this model may be seen as the analysis of a limiting case: the implications of the most simple model for the dynamics of SGS fluctuations are investigated in this way. This model will be used in Section 3 to derive closed LES equations for the velocity field. The reduction of the velocity-scalar FDF model to a scalar model, which can be applied in conjunction with the velocity LES model, will be performed in Section 4. The findings obtained will be summarized in Section 5.

2. The Closure of LES Equations

The LES equations will be presented in Section 2.1. Their closure requires their extension to a stochastic model. This will be presented in Section 2.2. Section 2.3 shows how this stochastic model can be reduced to consistent LES equations for the velocity field and scalar FDF transport equations. The realization of this reduction is then the concern of Sections 3 and 4.

2.1. THE LES EQUATIONS

The mass density-weighted filtered value of any function Q of velocities $\mathbf{U}(\mathbf{x}, t) = (U_1, U_2, U_3)$ and scalars (the mass fractions of N species and temperature) $\Phi(\mathbf{x}, t) = (\Phi_1, \dots, \Phi_{N+1})$ will be defined by

$$\bar{Q} = \langle \rho \rangle^{-1} \langle \rho Q \rangle. \quad (2.1)$$

Here, $\rho(\mathbf{x}, t)$ is written for the mass density, and the bracket refers to a spatial filtering,

$$\langle \rho(\mathbf{x}, t) Q(\mathbf{x}, t) \rangle = \int d\mathbf{r} \rho(\mathbf{x} - \mathbf{r}, t) Q(\mathbf{x} - \mathbf{r}, t) G(\mathbf{r}). \quad (2.2)$$

The filter function G is assumed to be homogeneous. We assume that $\int d\mathbf{r} G(\mathbf{r}) = 1$ and $G(\mathbf{r}) = G(-\mathbf{r})$. Moreover, only positive filter functions [41] are considered for which all the moments $\int d\mathbf{r} r^m G(\mathbf{r})$ exist for $m \geq 0$ [2].

The filtering of the basic equations results in the following LES equations for the filtered mass density $\langle \rho \rangle$, velocities \bar{U}_i and scalars $\bar{\Phi}_\alpha$,

$$\frac{\partial \langle \rho \rangle}{\partial t} + \frac{\partial \langle \rho \rangle \bar{U}_k}{\partial x_k} = 0, \quad (2.3a)$$

$$\begin{aligned} \frac{\partial \bar{U}_i}{\partial t} + \bar{U}_k \frac{\partial \bar{U}_i}{\partial x_k} + \langle \rho \rangle^{-1} \frac{\partial \langle \rho \rangle \overline{u_k u_i}}{\partial x_k} \\ = 2 \langle \rho \rangle^{-1} \frac{\partial}{\partial x_k} \langle \rho \rangle \nu \left(\bar{S}_{ik} - \frac{1}{3} \bar{S}_{mn} \delta_{ik} \right) - \langle \rho \rangle^{-1} \frac{\partial \langle p \rangle}{\partial x_i} + F_i, \end{aligned} \quad (2.3b)$$

$$\frac{\partial \bar{\Phi}_\alpha}{\partial t} + \bar{U}_k \frac{\partial \bar{\Phi}_\alpha}{\partial x_k} + \langle \rho \rangle^{-1} \frac{\partial \langle \rho \rangle \overline{u_k \phi_\alpha}}{\partial x_k} = \langle \rho \rangle^{-1} \frac{\partial}{\partial x_k} \langle \rho \rangle \nu_{(\alpha)} \frac{\partial \bar{\Phi}_\alpha}{\partial x_k} + \bar{S}_\alpha. \quad (2.3c)$$

Repeated indices imply summation with the exception of subscripts in parentheses. F_i is any external force (the acceleration due to gravity), $p = p(\rho, \Phi)$ the pressure that is defined via the thermal equation of state, and S_α denotes a known source rate. $S_{ik} = 1/2[\partial U_i/\partial x_k + \partial U_k/\partial x_i]$ is the rate-of-strain tensor and ν the kinematic viscosity, which is considered to be constant for simplicity. $\nu_{(\alpha)}$ is the molecular or thermal diffusivity of the scalar Φ_α . To derive the first term on the right-hand side of Equation (2.3b), we assumed that $\partial \bar{U}_i/\partial x_k = \partial \bar{U}_i/\partial x_k$. A corresponding relation is assumed regarding the derivation of the first term on the right-hand side of (2.3c). The expressions $\overline{u_k u_i}$ and $\overline{u_k \phi_\alpha}$ on the left-hand sides of (2.3b–2.3c) are called the SGS stress tensor and SGS scalar flux. Within the frame of RANS and PDF methods, one often considers u_i and ϕ_α to be the fluctuations of U_i and Φ_α . This is not done here but $\overline{u_k u_i}$ and $\overline{u_k \phi_\alpha}$ (and corresponding expressions that involve u_i and ϕ_α) are seen as symbols, which are defined by the following expanded forms:

$$\overline{u_k u_i} = \overline{U_k U_i} - \bar{U}_k \bar{U}_i, \quad \overline{u_k \phi_\alpha} = \overline{U_k \Phi_\alpha} - \bar{U}_k \bar{\Phi}_\alpha. \quad (2.4)$$

The purpose of defining $\overline{u_k u_i}$ and $\overline{u_k \phi_\alpha}$ in this way is to avoid the appearance of double-filtering operations $\bar{\bar{U}}_k$ and $\bar{\bar{\Phi}}_\alpha$ because $\bar{U}_k \neq \bar{\bar{U}}_k$ and $\bar{\Phi}_\alpha \neq \bar{\bar{\Phi}}_\alpha$ in general [33].

The problem that has to be solved to apply Equations (2.3a–2.3c) to turbulent reacting flow simulations is to provide closures for the unknowns $\overline{u_k u_i}$, $\overline{u_k \phi_\alpha}$ and \bar{S}_α . To calculate these terms, one has to assess the effects of fluctuations on $\overline{U_k U_i}$, $\overline{U_k \Phi_\alpha}$ and \bar{S}_α , which requires a model for both the dynamics of resolved variables \bar{U}_i , $\bar{\Phi}_\alpha$ and fluctuations around these variables. Such a model for the dynamics of instantaneous velocities and scalars will be presented next.

2.2. THE STOCHASTIC MODEL

The model for instantaneous velocities U_i^* ($i = 1, 3$) and scalars Φ_α^* ($\alpha = 1, N+1$) is considered within the Lagrangian framework, where particle positions x_i^* are involved as independent variables,

$$\frac{d}{dt} x_i^* = U_i^*, \quad (2.5a)$$

$$\frac{d}{dt}U_i^* = \bar{\Gamma}_i + \bar{F}_i - \frac{1}{\tau_L}(U_i^* - \bar{U}_i) + \sqrt{C_0\epsilon_r}\frac{dW_i}{dt}, \quad (2.5b)$$

$$\frac{d}{dt}\Phi_\alpha^* = \bar{\Omega}_\alpha + S_\alpha - \frac{1}{\tau_\varphi}(\Phi_\alpha^* - \bar{\Phi}_\alpha) + G_{\alpha m}(U_m^* - \bar{U}_m). \quad (2.5c)$$

$\bar{\Gamma}_i$ plus \bar{F}_i and $\bar{\Omega}_\alpha$ plus \bar{S}_α determine the dynamics of resolved velocities \bar{U}_i and scalars $\bar{\Phi}_\alpha$, as may be seen by filtering these equations. According to (2.3b–2.3c) one finds [13]

$$\begin{aligned} \bar{\Gamma}_i &= 2\langle\rho\rangle^{-1}\frac{\partial}{\partial x_k}\langle\rho\rangle v\left(\bar{S}_{ik} - \frac{1}{3}\bar{S}_{nn}\delta_{ik}\right) - \langle\rho\rangle^{-1}\frac{\partial\langle p\rangle}{\partial x_i}, \\ \bar{\Omega}_\alpha &= \langle\rho\rangle^{-1}\frac{\partial}{\partial x_k}\langle\rho\rangle v_{(\alpha)}\frac{\partial\bar{\Phi}_\alpha}{\partial x_k}. \end{aligned} \quad (2.6)$$

The body force in the velocity equation (2.5b) is assumed to be independent of velocities and scalars, $F_i = \bar{F}_i$. This simplifies the explanations given in Section 4 because \bar{F}_i does not affect the calculation of the SGS stress tensor. The Boussinesq approximation (see section 4.1 in Heinz [13]) is not covered in this way. There is no need for doing this because compressibility effects can be taken into account as shown in Section 3. No assumption is made regarding the source term S_α in the scalar equation (2.5c).

The remaining terms on the right-hand sides of (2.5b–2.5c) model the dynamics of velocity and scalar fluctuations. Velocity fluctuations are assumed to be generated by the last term in (2.5b). dW_i/dt is a Gaussian process with vanishing means, $\langle dW_i/dt \rangle = 0$, and uncorrelated values at different times, $\langle dW_i/dt(t) \cdot dW_j/dt'(t') \rangle = \delta_{ij}\delta(t-t')$. The symbol δ_{ij} is the Kronecker delta and $\delta(t-t')$ the delta function. The coefficient of dW_i/dt has the same structure as applied in PDF methods [33]. The SGS dissipation rate of turbulent kinetic energy ϵ_r will be defined in Section 3.1, and C_0 is a constant that has to be estimated. A corresponding stochastic source term in the scalar equation (2.5c) is not considered. Such a term is needed within the frame of PDF methods to simulate the loss of information about the initial PDF in time [13]. However, there is no need to consider such a term in FDF methods because most of the scalar spectrum is resolved. The effect of noise on the scalar dynamics is involved in (2.5c) via the term related to velocity fluctuations. The appearance of this term is a consequence of assuming a locally isotropic dissipation of the scalar field. Accordingly, $G_{\alpha m}$ is determined by [13]

$$G_{\alpha m} = \frac{1}{\tau_\varphi}\overline{\phi_\alpha u_i}V_{im}^{-1}. \quad (2.7)$$

V^{-1} refers to the inverse velocity variance matrix V which has elements $V_{ij} = \overline{u_i u_j}$. The third terms on the right-hand sides of (2.5b–2.5c) involve the most relevant assumptions. They model the relaxation of velocity and scalar fluctuations. It

is assumed here that velocity and scalar fluctuations relax only in interaction with their own means, where τ_L and τ_φ are characteristic relaxation times that have to be estimated.

Equations (2.5a–2.5c) for the dynamics of SGS fluctuations were validated through simulations of various two-dimensional jets and mixing layers and a three-dimensional temporally developing mixing layer. The good performance of the velocity equation (2.5b) (without body force) was proved by Gicquel et al. [8]. The performance of the scalar equation (2.5c) combined with a conventional LES equation for the velocity field was investigated by Colucci et al. [2], Jaber et al. [15] and Zhou and Pereira [45]. The term that involves velocity fluctuations in (2.5c) had to be neglected in these simulations because velocity fluctuations were not incorporated into the stochastic model. The consideration of the equations (2.5a–2.5c) can also be justified with the argument that their analysis is equivalent to the consideration of a limiting case: the equations (2.5a–2.5c) represent the simplest possible model for the dynamics of SGS fluctuations that can be applied.

It is worth emphasizing that the solution of (2.5a–2.5c) overcomes the closure problems related to the LES equations (2.3a–2.3c). Equations (2.5a–2.5c) are closed for specified τ_L , τ_φ and C_0 (which will be determined in Sections 3 and 4), and the expressions (2.6) assure that the transport of filtered quantities is calculated according to (2.3a–2.3c). However, the solution of (2.5a–2.5c) is very expensive. Thus, for reasons given in the introduction these equations will be reduced to simpler methods. The basic scheme of this reduction to be performed in Sections 3 and 4 will be outlined next.

2.3. THE CLOSURE OF LES EQUATIONS

The stochastic model presented above determines the joint velocity-scalar FDF that is defined by

$$F(\mathbf{v}, \boldsymbol{\theta}, \mathbf{x}, t) = \overline{\delta(\mathbf{U}(\mathbf{x}, t) - \mathbf{v})\delta(\boldsymbol{\Phi}(\mathbf{x}, t) - \boldsymbol{\theta})}. \quad (2.8)$$

Its transport equation can be derived from Equations (2.5a–2.5c) by means of standard methods. It reads [6, 33, 35]

$$\begin{aligned} & \frac{\partial}{\partial t} \langle \rho \rangle F + \frac{\partial}{\partial x_i} \langle \rho \rangle v_i F \\ &= - \frac{\partial}{\partial v_i} \langle \rho \rangle \left[\bar{\Gamma}_i - \frac{1}{\tau_L} (v_i - \bar{U}_i) + \bar{F}_i \right] F + \frac{\partial^2}{\partial v_j \partial v_j} \langle \rho \rangle \frac{C_0 \epsilon_r}{2} F \\ & \quad - \frac{\partial}{\partial \theta_\alpha} \langle \rho \rangle \left[\bar{\Omega}_\alpha - \frac{1}{\tau_\varphi} (\theta_\alpha - \bar{\Phi}_\alpha) + G_{\alpha m} (v_m - \bar{U}_m) + S_\alpha \right] F. \end{aligned} \quad (2.9)$$

By multiplying (2.9) with $v_i v_j$ and integrating it over the velocity-scalar space, one may derive the following equation for the SGS stress tensor $\overline{u_i u_j}$,

$$\begin{aligned} \frac{\partial \overline{u_i u_j}}{\partial t} + \bar{U}_k \frac{\partial \overline{u_i u_j}}{\partial x_k} + \langle \rho \rangle^{-1} \frac{\partial \langle \rho \rangle \overline{u_k u_i u_j}}{\partial x_k} + \overline{u_k u_j} \frac{\partial \bar{U}_i}{\partial x_k} + \overline{u_k u_i} \frac{\partial \bar{U}_j}{\partial x_k} \\ = -\frac{2}{\tau_L} \overline{u_i u_j} + C_0 \epsilon_r \delta_{ij}. \end{aligned} \quad (2.10)$$

In an analogous manner as the SGS stress tensor, the term $\overline{u_k u_i u_j}$ is defined by

$$\overline{u_k u_i u_j} = \bar{U}_k \bar{U}_i \bar{U}_j - \bar{U}_k \bar{U}_i \bar{U}_j - \bar{U}_k \overline{u_i u_j} - \bar{U}_i \overline{u_k u_j} - \bar{U}_j \overline{u_k u_i}, \quad (2.11)$$

where the first part of (2.4) has to be applied on the right-hand side. Equation (2.10) will be reduced in Section 3 to an algebraic model for the SGS stress tensor $\overline{u_i u_j}$ in order to close the velocity LES equation (2.3b).

In the framework of a model that provides only filtered velocities \bar{U}_i and not instantaneous velocities, (2.9) is not the appropriate FDF equation. Rather one has to reduce (2.9) to a closed equation for the scalar FDF $F_\varphi(\boldsymbol{\theta}, \mathbf{x}, t) = \overline{\delta(\boldsymbol{\Phi}(\mathbf{x}, t) - \boldsymbol{\theta})}$. The transport equation for F_φ can be obtained by integrating (2.9) over the velocity space. This results in

$$\begin{aligned} \frac{\partial}{\partial t} \langle \rho \rangle F_\varphi = & -\frac{\partial}{\partial x_i} \langle \rho \rangle (\bar{U}_i + \overline{u_i | \boldsymbol{\theta}}) F_\varphi \\ & - \frac{\partial}{\partial \theta_\alpha} \langle \rho \rangle \left[\bar{\Omega}_\alpha - \frac{1}{\tau_\varphi} (\theta_\alpha - \bar{\Phi}_\alpha) + G_{\alpha m} \overline{u_m | \boldsymbol{\theta}} + S_\alpha \right] F_\varphi. \end{aligned} \quad (2.12)$$

The closure of Equation (2.12) requires the determination of the scalar-conditioned convective flux

$$\overline{u_i | \boldsymbol{\theta}} = F_\varphi^{-1} \overline{U_i \delta(\boldsymbol{\Phi} - \boldsymbol{\theta})} - \bar{U}_i, \quad (2.13)$$

which is defined by the right-hand side. This quantity will be calculated in Section 4. The reduction of the velocity-scalar FDF transport equation (2.9) to closed equations (2.3b) and (2.12) is called a hybrid method.

The completion of this method to closed LES equations for velocities and scalars requires closure models for $\overline{u_i \phi_\alpha}$ and \bar{S}_α , which appear as unknowns in (2.3c). The hybrid method solves this problem regarding to $\overline{u_i \phi_\alpha}$. We may multiply (2.13) by $F_\varphi \theta_\alpha$ and perform the integration over the scalar space. This results in $\overline{u_i \phi_\alpha}$ provided the scalar-conditioned convective flux is known. A closure model for the filtered source rate \bar{S}_α in (2.3c) requires the knowledge of an analytical scalar FDF. Then, \bar{S}_α can be obtained by integration,

$$\bar{S}_\alpha = \int d\boldsymbol{\theta} S_\alpha(\boldsymbol{\theta}) F_\varphi(\boldsymbol{\theta}, \mathbf{x}, t). \quad (2.14)$$

The conditions for the existence of such an explicit expression for the scalar FDF F_φ will be pointed out in Section 4.

3. The Closure of the Equation for Filtered Velocities

Equation (2.10) for the SGS stress tensor will be reformulated in Section 3.1. The general algebraic solution to this equation is given in Section 3.2. In Section 3.3, this solution will be simplified to models for the SGS stress tensor which are linear and quadratic in the resolved shear tensor \bar{S}_{ik} . The relevance of quadratic contributions to the SGS stress tensor will be studied in Section 3.4 by means of a scaling analysis. Section 3.5 deals with the calculation of parameters that appear in the SGS stress tensor models by means of theoretical arguments. The validity of these findings will be investigated in Section 3.6 by comparisons with DNS data.

3.1. TRANSPORT EQUATION FOR THE SGS STRESS TENSOR

It is convenient for the following developments to split the SGS stress tensor $\overline{u_i u_j}$ into the anisotropic residual stress tensor

$$\tau_{ij} = \overline{u_i u_j} - \frac{2}{3}k_r \delta_{ij} \quad (3.1)$$

and its isotropic part $2k_r/3\delta_{ij}$, which is determined by the residual kinetic energy $k_r = \overline{u_j u_j}/2$. Equation (2.10) provides transport equations for τ_{ij} and k_r which read

$$\begin{aligned} \frac{\partial \tau_{ij}}{\partial t} + \bar{U}_k \frac{\partial \tau_{ij}}{\partial x_k} + \langle \rho \rangle^{-1} \frac{\partial \langle \rho \rangle \overline{u_k (u_i u_j - u_l u_l \delta_{ij}/3)}}{\partial x_k} \\ = -\frac{\partial \bar{U}_i}{\partial x_k} \tau_{kj} - \frac{\partial \bar{U}_j}{\partial x_k} \tau_{ki} - \frac{4}{3}k_r \bar{S}_{ij} - \frac{2}{\tau_L} \tau_{ij} - \frac{2}{3}P_r \delta_{ij}, \end{aligned} \quad (3.2a)$$

$$\frac{\partial k_r}{\partial t} + \bar{U}_k \frac{\partial k_r}{\partial x_k} + \frac{1}{2} \langle \rho \rangle^{-1} \frac{\partial \langle \rho \rangle \overline{u_k u_l u_l}}{\partial x_k} = P_r - \epsilon_r. \quad (3.2b)$$

$P_r = -\overline{u_i u_j} \bar{S}_{ji}$ is the production rate of residual kinetic energy, and the dissipation rate ϵ_r is given by $\epsilon_r = 2k_r / [(1 + 1.5C_0)\tau_L]$. The model (3.2a–3.2b) determines the SGS stress tensor provided that τ_L and C_0 are given, and the $\overline{u_k u_l u_l}$ expressions are closed. The latter can be achieved by means of the transport equation for $\overline{u_k u_l u_l}$, which follows from (2.9).

3.2. GENERAL ALGEBRAIC EXPRESSION FOR THE SGS STRESS TENSOR

To derive an algebraic expression for the SGS stress tensor we neglect the left-hand sides of Equations (3.2a–3.2b) in comparison to the terms on the right-hand sides. This results in

$$\begin{aligned} B_{ik}^* \left(S_{kj}^* - \Sigma_{kj}^* + \frac{1}{2} \delta_{kj} \right) + B_{jk}^* \left(S_{ki}^* - \Sigma_{ki}^* + \frac{1}{2} \delta_{ki} \right) \\ = -S_{ij}^* + \frac{2}{3} B_{kl}^* S_{lk}^* \delta_{ij}, \end{aligned} \quad (3.3a)$$

$$B_{kl}^* S_{lk}^* = -\frac{3}{4} \left(1 - \frac{1}{1 + \tau_L \bar{S}_{nn}/3} \frac{C_0}{C_0 + 2/3} \right), \quad (3.3b)$$

where the abbreviations

$$\begin{aligned} B_{ij}^* &= \frac{3}{4} \frac{\tau_{ij}}{k_r}, & S_{ij}^* &= \frac{\tau_L}{2} \frac{1}{1 + s\tau_L \bar{S}_{nn}/3} \left(\bar{S}_{ij} - \frac{1}{3} \bar{S}_{nn} \delta_{ij} \right), \\ \Sigma_{ij}^* &= \frac{\tau_L}{2} \frac{1}{1 + \tau_L \bar{S}_{nn}/3} \bar{\Sigma}_{ij} \end{aligned} \quad (3.4)$$

are used. Here, $\Sigma_{ij} = 1/2[\partial U_i/\partial x_j - \partial U_j/\partial x_i]$ denotes the rate-of-rotation tensor. Relation (3.3b) follows from the definition $P_r = -\bar{u}_i \bar{u}_j \bar{S}_{ji}$ in conjunction with $P_r = \epsilon_r = 2k_r/[(1 + 1.5C_0)\tau_L]$, which is implied by (3.2b).

There are different ways to solve (3.3a) exactly (see [35, p. 155]), but the presentation of its solution by means of an integrity basis is most convenient because it allows explicit comparisons with other methods. For that, we restrict the development to the consideration of an incompressible flow. This allows the use of a technique that was developed by Pope [30] and applied by Gatski and Speziale [7]. Nevertheless, the explanations given below show that the incorporation of compressibility effects is straightforward. The general solution of (3.3a) may be written as

$$B^* = \sum_{\lambda=1}^9 G^{(\lambda)} T^{(\lambda)}. \quad (3.5)$$

The integrity basis $T^{(\lambda)}$ and coefficients $G^{(\lambda)}$ are given in Table I. In the relations for the coefficients $G^{(\lambda)}$ one finds the following irreducible invariants of S^* and Σ^* ,

$$\begin{aligned} \eta_1 &= \{S^{*2}\}, & \eta_2 &= \{\Sigma^{*2}\}, & \eta_3 &= \{S^{*3}\}, \\ \eta_4 &= \{S^* \Sigma^{*2}\}, & \eta_5 &= \{S^{*2} \Sigma^{*2}\}. \end{aligned} \quad (3.6)$$

The denominator D in the expressions for $G^{(\lambda)}$ is a function of these invariants,

$$\begin{aligned} D &= 3 - 3.5\eta_1 + \eta_1^2 - 7.5\eta_2 - 8\eta_1\eta_2 + 3\eta_2^2 - \eta_3 + 1.5\eta_1\eta_3 \\ &\quad - 2\eta_2\eta_3 + 21\eta_4 + 24\eta_5 + 2\eta_1\eta_4 - 6\eta_2\eta_4. \end{aligned} \quad (3.7)$$

An important property of the algebraic model obtained is that the relation (3.3b), which represents the algebraic k_r -equation (3.2b), provides an equation of sixth-order for τ_L ,

$$\begin{aligned} \frac{D}{C_0 + 2/3} &= \eta_1(6 - 3\eta_1 - 21\eta_2 + 4\eta_3 + 12\eta_4) \\ &\quad - 2\eta_3(6 - 2\eta_3 - 12\eta_4) + 36\eta_4^2 + 36\eta_5, \end{aligned} \quad (3.8)$$

Table I. The integrity basis and coefficients that appear in the relation (3.5). $\{\cdot\}$ denotes the trace and I being the unity tensor. The invariants η_1 – η_5 are given by (3.6) and D by (3.7).

$T^{(1)} = S^*$	$G^{(1)} = -(6 - 3\eta_1 - 21\eta_2 - 2\eta_3 + 30\eta_4)/(2D)$
$T^{(2)} = S^* \Sigma^* - \Sigma^* S^*$	$G^{(2)} = -(3 + 3\eta_1 - 6\eta_2 + 2\eta_3 + 6\eta_4)/D$
$T^{(3)} = S^{*2} - \{S^{*2}\}I/3$	$G^{(3)} = (6 - 3\eta_1 - 12\eta_2 - 2\eta_3 - 6\eta_4)/D$
$T^{(4)} = \Sigma^{*2} - \{\Sigma^{*2}\}I/3$	$G^{(4)} = -3(3\eta_1 + 2\eta_3 + 6\eta_4)/D$
$T^{(5)} = \Sigma^* S^{*2} - S^{*2} \Sigma^*$	$G^{(5)} = -9/D$
$T^{(6)} = \Sigma^{*2} S^* + S^* \Sigma^{*2} - 2\{S^* \Sigma^{*2}\}I/3$	$G^{(6)} = -9/D$
$T^{(7)} = \Sigma^* S^* \Sigma^{*2} - \Sigma^{*2} S^* \Sigma^*$	$G^{(7)} = 9/D$
$T^{(8)} = S^* \Sigma^* S^{*2} - S^{*2} \Sigma^* S^*$	$G^{(8)} = 9/D$
$T^{(9)} = \Sigma^{*2} S^{*2} + S^{*2} \Sigma^{*2} - 2\{S^{*2} \Sigma^{*2}\}I/3$	$G^{(9)} = 18/D$

whereas k_r is unconstrained in that algebraic approximation. We have to define τ_L as a function of k_r in order to transform (3.8) into an equation for k_r . This is done by assuming $\tau_L = \ell/k_r^{1/2}$, where a length scale ℓ is introduced. Further, we scale ℓ by $\ell = \ell_* \Delta$, where ℓ_* is a number and Δ the filter width. Hence, we find the SGS stress tensor in dependence on the parameters C_0 and ℓ_* . The relation of the algebraic model (3.5) to models applied usually will be considered next.

3.3. LINEAR AND QUADRATIC ALGEBRAIC SGS STRESS TENSOR MODELS

First, we consider the simplest version of (3.5) where only shear of first-order is taken into account. In this first approximation we find $B_{(1)}^* = -S^*$. This may be written in terms of τ_{ij} as

$$\tau_{ij}^{(1)} = -2\nu_r \bar{S}_{ij}, \quad (3.9)$$

where the residual eddy viscosity $\nu_r = k_r \tau_L/3$ is introduced. Relation (3.9) may also be obtained by neglecting the production in (3.3a), i.e., the first-, second-, fourth- and fifth-term on the left-hand side, and the last term on the right-hand side. Equation (3.8) provides then

$$k_r^{(1)} = \frac{1 + 1.5 C_0}{6} \ell_*^2 \Delta^2 |\bar{S}|^2, \quad (3.10)$$

where $|\bar{S}| = \sqrt{2\bar{S}_{kl}\bar{S}_{lk}}$. This expression for k_r may be proved by equating ϵ_r with the production P_r that follows from the use of (3.9). The use of (3.10) in (3.9) provides then

$$\tau_{ij}^{(1)} = -2c_S \Delta^2 |\bar{S}| \bar{S}_{ij}, \quad (3.11)$$

where the parameter c_S is introduced, which is given by

$$c_S = \sqrt{\frac{1 + 1.5 C_0}{54}} \ell_*^2 \ell_*. \quad (3.12)$$

The comparison of (3.11) with the Smagorinsky model reveals that c_S corresponds to the Smagorinsky coefficient. c_S can be calculated by adopting a dynamic procedure that is given by the expression (A.4) in Appendix A.

This dynamic Smagorinsky model is capable of describing backscatter, which refers to the appearance of locally negative values of the production $P_r = -\tau_{ij}^{(1)} \bar{S}_{ji} = c_S \Delta^2 |\bar{S}|^3$ [20, 23, 29]. A requirement for the inclusion of backscatter is the consideration of locally negative values of ℓ_* , which has significant consequences regarding the approach presented here: it corresponds to the consideration of locally negative time scales $\tau_L = \ell_* \Delta / k_r^{1/2}$. The latter extends significantly concepts used previously for stochastic turbulence simulations, but it is physically plausible. The appearance of linear velocity terms with negative frequencies can be interpreted as stochastic forcing in addition to the last term in (2.5b). Obviously, the necessary condition for the acceptability of such terms is that the mean of τ_L is always positive.

In the next order of approximation, we consider shear-contributions up to second-order in (3.5), which results in $B_{(2)}^* = -S^* - (S^* \Sigma^* - \Sigma^* S^*) + 2(S^{*2} - \{S^{*2}\}I/3)$, or,

$$\begin{aligned} \tau_{ij}^{(2)} = & -2\nu_r \bar{S}_{ij} - \nu_r \tau_L (\bar{S}_{ik} \bar{\Sigma}_{kj} - \bar{\Sigma}_{ik} \bar{S}_{kj}) \\ & + 2\nu_r \tau_L \left(\bar{S}_{ik} \bar{S}_{kj} - \frac{1}{3} \bar{S}_{nk} \bar{S}_{kn} \delta_{ij} \right). \end{aligned} \quad (3.13)$$

This expression follows from (3.3a) if B^* is replaced in the production terms by $-S^*$ according to the first approximation. Equation (3.8) (or the equality of ϵ_r with the production P_r that follows from the use of (3.13)) now results in the following expression for k_r ,

$$k_r^{(2)} = \frac{1 + 1.5 C_0}{6} \kappa^2 \ell_*^2 \Delta^2 |\bar{S}|^2. \quad (3.14)$$

Here we introduced the positive variable κ that is given as the solution of a third-order equation,

$$0 = \kappa^3 - \kappa + s_*. \quad (3.15)$$

The last term in (3.15) is given by $s_* = \lambda s$, where $\lambda = \sqrt{27/(8 + 12C_0)}$ and $s = (\ell_*/|\ell_*|) \text{III}_S / (-\text{II}_S)^{3/2}$ are introduced. s is similar to the generalized skewness function used by Kosović [17] and defined in terms of the invariants $\text{II}_S = -|\bar{S}|^2/4$ and $\text{III}_S = \{\bar{S}^3\}/3$ [21]. The variation of κ is illustrated in Figure 1 which shows all the positive solutions of (3.15). Their existence requires that $s_* \leq 2/\sqrt{27}$. The dashed curve for $\kappa \leq 1/\sqrt{3}$ is found to be unphysical because it is inconsistent with $\kappa = 1$ at $s_* = 0$. The solid curve is given by the relation $\kappa = 2 \cos(\varphi/3)/\sqrt{3}$, where φ is defined through $\cos(\varphi) = -1.5\sqrt{3}s_*$.

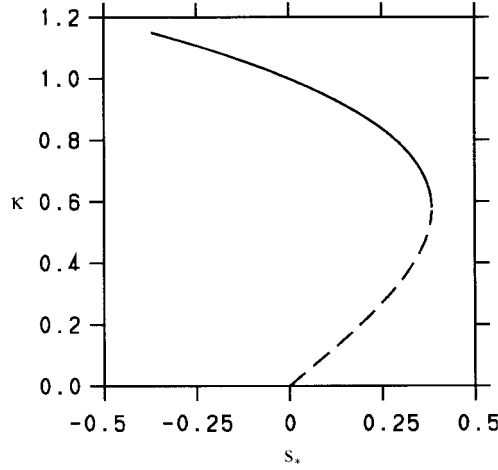


Figure 1. κ in dependence on s_* according to Equation (3.15).

To compare (3.13) with other findings we rewrite it by means of the definitions of \bar{S}_{ij} and $\bar{\Sigma}_{ij}$

$$\begin{aligned} \tau_{ij}^{(2)} = & -2\kappa c_S \Delta^2 |\bar{S}| \bar{S}_{ij} + \frac{\ell_*^2 \Delta^2}{3} \left[\frac{\partial \bar{U}_i}{\partial x_k} \frac{\partial \bar{U}_j}{\partial x_k} - \frac{\delta_{ij}}{3} \frac{\partial \bar{U}_l}{\partial x_k} \frac{\partial \bar{U}_l}{\partial x_k} \right. \\ & \left. + \frac{1}{2} \left(\frac{\partial \bar{U}_i}{\partial x_k} \frac{\partial \bar{U}_k}{\partial x_j} + \frac{\partial \bar{U}_j}{\partial x_k} \frac{\partial \bar{U}_k}{\partial x_i} \right) - \frac{\delta_{ij}}{3} \frac{\partial \bar{U}_l}{\partial x_k} \frac{\partial \bar{U}_k}{\partial x_l} \right]. \end{aligned} \quad (3.16)$$

It is worth emphasizing that the justification for the expression (3.16) obtained for the SGS stress tensor arises from the fact that it is implied by the stochastic model (2.5a–2.5c). The available support for (2.5a–2.5c) was described in Section 2.2. Further, it was pointed out that the consideration of (2.5a–2.5c) corresponds to the consideration of the simplest possible model for the physics of SGS fluctuations. Consequently, (3.16) represents the simplest model for the SGS stress tensor if one includes shear up to second-order. The advantage of (3.16) compared to existing models of this type is given through its consistency. First, this concerns the consistent consideration of quadratic shear terms. The model of Clark et al. [1], for instance, is generalized due to the appearance of the last two terms inside the bracket (and the pre-factor, which is calculated here in dependence on ℓ_* whereas Clark's model assumes a fixed value $\ell_* = 0.5$). Second, this concerns the consistent calculation of the coefficients of linear and quadratic terms. It is of interest to note that the model (3.16) has the same structure as the model applied by Kosović [17]. However, the latter model applies coefficients of quadratic contributions which are estimated by a heuristic argument and vanish under conditions where backscatter is negligible. In contrast to this, the coefficients of (3.16) are explained (for both the case that backscatter is relevant or not) as functions of the two parameters C_0 and ℓ_* of the velocity model (2.5b). For C_0 , a theoretical value will be derived

in Section 3.5. The remaining parameter ℓ_* can be estimated then by means of the dynamic procedure (A.1) presented in Appendix A. This makes it possible to perform self-consistent flow simulations.

3.4. SCALING ANALYSIS

An important question concerns the relevance of quadratic shear contributions in the expression (3.13) for the SGS stress tensor. To address this question, we apply (in analogy to the assessment of the relevance of nonlinear shear contributions to the stress tensor in the basic equations) a scaling analysis. We scale τ_{ij} in terms of a characteristic velocity scale U_0 and L_0 which characterizes the spatial scale of the flow considered. The rescaled expression (3.13) then reads

$$\begin{aligned} \tau_{ij}^+ &= -i_r \text{Kn}_r \bar{S}_{ij}^+ \\ &+ \text{Kn}_r^2 \left\{ \bar{S}_{ik}^+ \bar{S}_{kj}^+ - \frac{1}{3} \{\bar{S}^+ \bar{S}^+\} \delta_{ij} - \frac{1}{2} (\bar{S}_{ik}^+ \bar{\Sigma}_{kj}^+ - \bar{\Sigma}_{ik}^+ \bar{S}_{kj}^+) \right\}. \end{aligned} \quad (3.17)$$

The plus refers to scaled quantities of order unity. This means the scaled anisotropic residual SGS stress tensor is given by $\tau_{ij}^+ = \tau_{ij}^{(2)}/U_0^2$, the scaled rate-of-strain tensor by $\bar{S}_{ik}^+ = \bar{S}_{ik} L_0/U_0$, and the scaled rate-of-rotation tensor by $\bar{\Sigma}_{kj}^+ = \bar{\Sigma}_{kj} L_0/U_0$. Further, two dimensionless numbers are used in (3.17), the SGS Knudsen number Kn_r and turbulence intensity i_r . These parameters are given by

$$\text{Kn}_r = \sqrt{\frac{2}{3}} \frac{\ell}{L_0}, \quad i_r = \frac{1}{U_0} \sqrt{\frac{2k_r}{3}} = \sqrt{\frac{1 + 1.5C_0}{6}} \kappa |\bar{S}|^+ |\text{Kn}_r|. \quad (3.18)$$

The consideration of the factor $\sqrt{2/3}$ in Kn_r simplifies the writing of (3.17) and the following discussion. The last term for i_r follows from the use of (3.14). The expression (3.17) confirms previous conclusions about the significance of quadratic shear contributions [17, 18, 43]. i_r and Kn_r are of the same order of magnitude in general so that the quadratic terms in (3.17) cannot be neglected in comparison to the linear term.*

Nevertheless, it is essential to note that the relevance of quadratic shear contributions to flow simulations depends significantly on the value of Kn_r . One may differentiate three cases in dependence on the setting of Kn_r (which can be chosen through the numerical resolution of the flow). The first case is given for very small

* This finding is significantly different to the result that follows from the consideration of the same problem at the molecular level. In correspondence to (3.17), one may derive an expression for the stress tensor in the basic equations from the molecular dynamics. This expression is given by replacing Kn_r by $2\sqrt{\gamma}\text{Kn}$ and i_r by $1/(\sqrt{\gamma}\text{Ma})$ in (3.17). Here, Kn is the Knudsen number, Ma the Mach number and γ the ratio of the constant-pressure to constant-volume specific heats. These relations explain the difference of the significance of quadratic shear contributions in basic equations and filtered equations. One often has the case that $1/\text{Ma}$ is much larger than Kn , whereas i_r and Kn_r are found to be of the same order of magnitude in general.

values of Kn_r (less than about 0.004 for the conditions considered by Gicquel et al. [8]): the contribution of the SGS stress tensor model is about 2×10^{-5} times smaller than other contributions in (2.3b), i.e., it is irrelevant. The second case is given for small values of Kn_r (near 0.03 regarding the studies of Gicquel et al. [8]): the details of the SGS stress tensor model are of minor relevance to flow simulations in this case so that the neglect of quadratic shear contributions can be compensated by dynamic adjustments of ℓ_* . The third case is given if Kn_r becomes larger than about 0.03. The details of the SGS stress tensor model become then essential, this means quadratic shear contributions have to be involved, in particular, regarding to simulations of significantly anisotropic flows.

3.5. THEORETICAL CALCULATION OF PARAMETERS

Another question related to the analysis of (3.13) concerns the calculation of the model parameters C_0 and ℓ_* . This will be addressed first with reference to C_0 . For that, let us have a closer look at the calculation of the standardized SGS kinetic energy κ via (3.15). The variation of $s_* = \lambda s$ shown in Figure 1 has to be explained through its s -dependence because λ is considered as a constant. In particular, we have the constraint $2/\sqrt{27} = s_*^{\max} = \lambda s^{\max}$, where s_*^{\max} and s^{\max} are the maximal values of s_* and s . To calculate s^{\max} , we may assume that ℓ_* is positive and consider the possible range of values of s . The invariants III_S and II_S are the same in every coordinate system, i.e., we may consider \bar{S}_{ij} in principal axes where the off-diagonal elements are zero. Due to the assumed $\bar{S}_{nn} = 0$, \bar{S}_{ij} is then a function of two independent components. A simple analysis of $\text{III}_S/(-\text{II}_S)^{3/2}$ as function of these two variables shows that [21]

$$-\frac{2}{\sqrt{27}} \leq s \leq \frac{2}{\sqrt{27}}. \quad (3.19)$$

By adopting (3.19) in $2/\sqrt{27} = \lambda s^{\max}$, we find $\lambda = \sqrt{27/(8 + 12C_0)} = 1$, which corresponds to

$$C_0 = \frac{19}{12}. \quad (3.20)$$

This value has to be seen as the asymptotic value of C_0 regarding the simulation of high-Reynolds number turbulence by means of FDF methods. It is of interest to note that the result $C_0 \approx 1.58$ obtained here agrees well with corresponding values used for C_0 within the frame of PDF methods. One often applies C_0 values in between 1 and 3 to simulate inhomogeneous and anisotropic flows at high-Reynolds numbers [3, 10, 11].

The non-dimensional length scale ℓ_* may be calculated as a function of fluctuating velocities and velocity gradients (filtered at different levels) if the dynamic procedure (A.1) given in Appendix A is applied for its calculation. In this case, ℓ_* varies with different realizations of the turbulent flow considered. An alternative

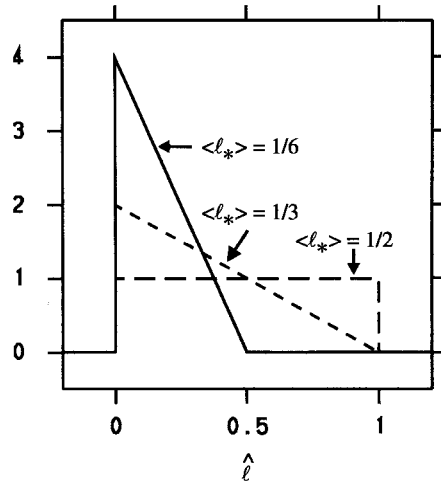


Figure 2. A range of idealized PDF shapes of the non-dimensional length scale l_* in sample space \hat{l} . The corresponding mean values, $\langle l_* \rangle = 1/2, 1/3$ and $1/6$, are shown with reference to their PDF.

to this approach is the use of a mean value for l_* [8], which corresponds to the application of a constant c_S in LES. The estimation of such an optimal value for l_* requires an assessment of possible variations of l_* . This question will be addressed now. l_* may be seen as a standardized fluctuating eddy length. According to Kolmogorov's theory, one should expect a distribution of eddy lengths with a higher probability for the appearance of small eddies. In particular, the eddy lengths PDF should approach to zero for values of l_* near unity. This assumption results in the PDF given with the mean $l_* = 1/3$ in Figure 2. This figure also presents two further PDFs in order to illustrate the range of variations of the eddy lengths PDF. The upper limiting PDF shape is given through the assumption of a uniform eddy lengths PDF. Therefore, Figure 2 suggests the following range of l_* variations that may be expected,

$$l_* = \frac{1}{3} \left(1 \pm \frac{1}{2} \right). \quad (3.21)$$

One way to prove the suitability of these estimates for C_0 and l_* is to have a look at the implications for the Smagorinsky constant c_S . The use of (3.20) and (3.21) in (3.12) implies $c_S^{1/2} = 0.17 \pm 0.08$, which agrees well with values applied usually [33]. The calculation of c_S provided here enables also the assessment of the relation between C_0 with the Kolmogorov constant C_K that determines the energy spectrum. For that, we set according to (3.21) $l_* = 2(8/19)^{3/4}/\pi$ in (3.12) and adopt Lilly's classical result $c_S^{1/2} = \pi^{-1}[2/(3C_K)]^{3/4}$ [19]. This leads to the relation

$$C_K = \frac{19}{12} \left(\frac{27}{8 + 12C_0} \right)^{1/3}. \quad (3.22)$$

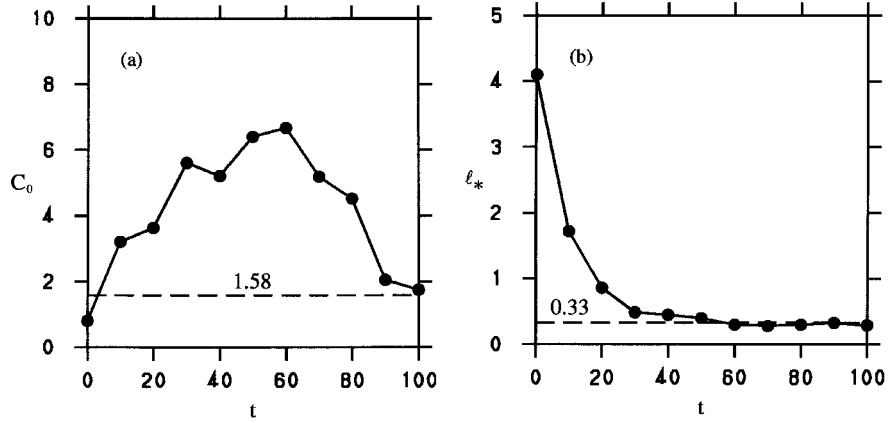


Figure 3. The calculation of C_0 and l_* (as functions of the normalized time t) by means of the DNS data reported by Gicquel et al. [8]. The values $C_0 = 19/12$ and $l_* = 0.33$ obtained in Section 3.5 by theoretical arguments are shown for a comparison.

By adopting (3.20), we find that the bracket factor in (3.22) is unity. This implies that C_0 and C_K are equal, $C_K = C_0 = 19/12 \approx 1.58$. This result for C_K agrees very well with results of measurements, which provide $C_K = 55/18(0.53 \pm 0.055) = 1.62 \pm 0.17$ [40].

3.6. COMPARISON WITH DNS DATA

Next, we compare (3.20) and (3.21) for C_0 and l_* with available DNS data. This can be done by means of the results of Gicquel et al. [8]. In terms of their notation, C_0 and l_* are given by $C_0 = 2(\tilde{C}_1 - 1)/3$ and $l_* = 2/(\tilde{C}_1 \tilde{C}_\epsilon)$. The values obtained for these parameters are presented in Figure 3.

The C_0 curve reveals two different stages. For $t < 50$, the flow evolves from an initially smooth laminar state to a three-dimensional turbulent state before the action of the small scales becomes significant [8]. Values of C_0 around 6 at $t \approx 50$ are consistent with experience obtained within the frame of PDF methods for flows of low complexity as stationary homogeneous isotropic turbulence [32, 38, 39]. For $t > 50$, the typical flow structures of the mixing layer considered develop [8]. C_0 approaches asymptotically to $C_0 = 19/12$, this means the theoretical finding (3.20) is well supported by these DNS results. The l_* curve is approximately constant for $t > 50$ and found in a very good agreement with the theoretical estimate $l_* = 1/3$.

It is worth emphasizing that these a priori DNS calculations of C_0 and l_* are well supported by corresponding a posteriori results of Gicquel et al. [8], where the effects of C_0 and l_* variations on flow simulations were investigated. These findings reveal that the use of values near $C_0 = 2.1$ and $l_* = 0.5$ results in satisfactory predictions [8]. In particular, it was found that l_* should not be taken larger than $l_* = 0.5$, which agrees very well with the implications of (3.21).

4. The Closure of the Equation for Filtered Scalars

We turn to the calculation of scalar transport. According to the explanations given in Section 2.3, this requires the closure of the convective flux $\overline{u_i | \theta}$ in the scalar FDF equation (2.12). This will be done in Section 4.1 and further discussed in Section 4.2. Section 4.3 deals with a discussion of the parametrization of the scalar mixing frequency τ_φ^{-1} , which has to be provided to close (2.12).

4.1. THE SCALAR-CONDITIONED CONVECTIVE FLUX

As noted in Section 2.3, in the framework of a model that provides only filtered velocities \bar{U}_i and not instantaneous velocities, (2.9) is not the appropriate FDF equation. Rather one has to reduce the joint velocity-scalar FDF equation (2.9) to the scalar FDF transport equation (2.12). This equation is unclosed due to the appearance of the scalar-conditioned convective flux $\overline{u_i | \theta}$. The calculation of this quantity from the underlying velocity-scalar FDF transport equation is performed in Appendix B. This results in

$$\overline{u_i | \theta} F_\varphi = -K_{ik} \frac{\partial F_\varphi}{\partial x_k} \quad (4.1)$$

if counter-gradient terms are neglected, see the explanations given in Appendix B. The diffusion coefficient K_{ij} in (4.1) is given through

$$K_{ij} = \tau_L \gamma^{-1} \overline{u_n u_n u_j}, \quad (4.2)$$

where γ^{-1} is the inverse matrix of γ which has elements $\gamma_{ij} = \delta_{ij} + \tau_L \partial \bar{U}_i / \partial x_j$. The diffusion coefficient K_{ij} will be considered in more detail in Section 4.2. The use of (4.1) in (2.12) results in the following scalar FDF equation

$$\begin{aligned} \frac{\partial}{\partial t} \langle \rho \rangle F_\varphi = & - \frac{\partial}{\partial x_i} \langle \rho \rangle \left\{ \bar{U}_i F_\varphi - K_{im} \frac{\partial F_\varphi}{\partial x_m} \right\} \\ & - \frac{\partial}{\partial \theta_\alpha} \langle \rho \rangle \left\{ \left[\bar{\Omega}_\alpha - \frac{1}{\tau_\varphi} (\theta_\alpha - \bar{\Phi}_\alpha) + S_\alpha \right] F_\varphi - G_{\alpha n} K_{nm} \frac{\partial F_\varphi}{\partial x_m} \right\}. \end{aligned} \quad (4.3)$$

$G_{\alpha m}$ is given by (2.7), and the parametrization of the mixing frequency τ_φ^{-1} will be addressed below.

The solution of (4.3) permits to calculate the scalar transport in consistency with the transport equations for filtered scalars,

$$\frac{\partial \bar{\Phi}_\alpha}{\partial t} + \bar{U}_k \frac{\partial \bar{\Phi}_\alpha}{\partial x_k} = \langle \rho \rangle^{-1} \frac{\partial}{\partial x_k} \langle \rho \rangle (v_{(\alpha)} \delta_{km} + K_{km}) \frac{\partial \bar{\Phi}_\alpha}{\partial x_m} + \bar{S}_\alpha, \quad (4.4)$$

which follow from (4.3) through multiplication with θ_α and integration over the scalar space. The extension of (4.4) through (4.3) is a requirement to involve the effects of source rates S_α on $\bar{\Phi}_\alpha$ without further approximations. A simpler approach than the use of (4.3) to obtain the scalar FDF F_φ is the assumed-shape FDF

approach where an analytical form for F_φ is provided to calculate \bar{S}_α in (4.4) via (2.14). Usually, one assumes that F_φ only depends on $\bar{\Phi}_\alpha$ and the scalar variances $V_{\alpha\beta} = \overline{\phi_\alpha\phi_\beta}$. The $\bar{\Phi}_\alpha$ are then calculated according to (4.4), and the $V_{\alpha\beta}$ are parametrized [42] or calculated by their transport equation. This approach is simple and relatively effective, but its range of applicability is limited. This is shown in Appendix C. It is pointed out there that the assumption of an assumed shape for F_φ is justified if there are no velocity-scalar fluctuations, i.e., no production mechanism for scalar fluctuations. This assumption cannot be considered to be justified in general. Further, it is worth noting that the application of this approach requires the specification of the shape of the FDF F_φ . This poses a non-trivial problem: one has to provide a FDF-shape that covers both the initial and final stage of the FDF evolution. For these reasons, the solution of (4.3) represents a much more flexible method compared to the assumed-shape FDF approach.

4.2. THE DIFFUSION COEFFICIENT

Next, we will consider the properties of K_{ij} in more detail. By adopting (4.2) combined with the Smagorinsky model (3.11) for the SGS stress tensor, the diffusion coefficient K_{ij} is found to satisfy

$$(\delta_{in} + \tau_L \bar{S}_{in} + \tau_L \bar{\Sigma}_{in}) K_{nj} = 2\nu_r (\delta_{ij} - \tau_L \bar{S}_{ij}). \quad (4.5)$$

Here, $\tau_L = \ell_* \Delta / k_r^{1/2}$ and the residual eddy viscosity $\nu_r = k_r \tau_L / 3$. By adopting (3.10) one finds then

$$\nu_r = c_S \Delta^2 |\bar{S}|. \quad (4.6)$$

Therefore, in contrast to the usual assumption of an isotropic K_{ij} [2, 15, 45] one finds an anisotropic relation for it even when the simplest model for the SGS stress tensor is applied.

Relation (4.5) can be simplified in the case of small shear. In zeroth, first and second order of approximation, one finds

$$\begin{aligned} K_{ij}^{(0)} &= \frac{\nu_r}{Sc_t} \delta_{ij}, & K_{ij}^{(1)} &= \frac{\nu_r}{Sc_t} (\delta_{ij} - \tau_L \bar{S}_{ij}), \\ K_{ij}^{(2)} &= \frac{\nu_r}{Sc_t} (\delta_{in} - \tau_L \bar{S}_{in} - \tau_L \bar{\Sigma}_{in}) (\delta_{nj} - \tau_L \bar{S}_{nj}). \end{aligned} \quad (4.7)$$

Here, the turbulent Schmidt number Sc_t is given by

$$Sc_t = \frac{1}{2}, \quad (4.8)$$

which follows as a consequence of (4.5). This theoretical value (4.8) for Sc_t agrees very well with values $Sc_t = 0.55 \pm 0.15$ applied in scalar FDF methods [15].

We turn to the question about the relevance of shear contributions to the diffusion coefficient K_{ij} . For that, we apply the same scaling analysis as in Section 3.4.

By adopting again U_0 and L_0 as characteristic velocity and length scales, we obtain from (4.5) the relation

$$(i_r \delta_{in} + \text{Kn}_r \bar{S}_{in}^+ + \text{Kn}_r \bar{\Sigma}_{in}^+) K_{nj}^+ = i_r \text{Kn}_r (i_r \delta_{ij} - \text{Kn}_r \bar{S}_{ij}^+), \quad (4.9)$$

where the plus refers to scaled quantities ($K_{nj}^+ = K_{nj}/U_0 L_0$). The conclusion that can be drawn from (4.9) regarding the relevance of shear contributions is the same as obtained for τ_{ij} : such contributions are important in general. This is confirmed by studies of the anisotropy of K_{ij} performed by Rogers et al. [36] and Kaltenbach et al. [16]. These investigations show that K_{ij} is strongly anisotropic and asymmetric even for homogeneous turbulence. For unstratified shear flow one finds for instance for the diagonal elements of the diffusion coefficient that $K_{11}/K_{22} = 2.9$ and $K_{33}/K_{22} = 0.53$, and the nonzero off-diagonal elements are characterized by $K_{13}/K_{22} = -1.2$ and $K_{31}/K_{22} = -0.65$ [16].

4.3. THE SCALAR MIXING FREQUENCY

The effect of parametrizations of the mixing frequency τ_φ^{-1} can be seen at best by means of the scalar variance transport equation for an inert scalar (referred to without subscript). This equation reads according to (4.3)

$$\frac{\partial \bar{\phi}^2}{\partial t} + \bar{U}_k \frac{\partial \bar{\phi}^2}{\partial x_k} + \langle \rho \rangle^{-1} \frac{\partial \langle \rho \rangle u_k \bar{\phi}^2}{\partial x_k} = -2 \frac{1 - R}{\tau_\varphi} \bar{\phi}^2 - 2 \overline{u_k \phi} \frac{\partial \bar{\Phi}}{\partial x_k}. \quad (4.10)$$

Here, we used the abbreviation $R = r_k r_k$, where r_k is the correlation coefficient of velocity and scalar fluctuations, $r_k = V^{-1/2} \overline{u_m \phi} / \bar{\phi}^{1/2}$. A simple analysis reveals the range of R variations, $0 \leq R < 1$. The case $R = 1$ would correspond to a perfect correlation of the scalar considered with the velocity field. This case cannot be realized provided the intensity of the stochastic source term (C_0) in the velocity equation is positive definite.

The closure of (4.10) requires the calculation of velocity-scalar correlations. This can be achieved by means of (4.1) combined (in the first order of approximation) with $K_{ij}^{(0)}$ of (4.7) and $v_r = k_r \tau_L / 3 = \ell_*^2 \Delta^2 / (3\tau_L)$. One obtains

$$\overline{u_k \phi} = -2 \frac{\ell_*^2 \Delta^2}{3\tau_L} \frac{\partial \bar{\Phi}}{\partial x_k}, \quad \overline{u_k \phi^2} = -2 \frac{\ell_*^2 \Delta^2}{3\tau_L} \frac{\partial \bar{\phi}^2}{\partial x_k}. \quad (4.11)$$

The assumption of an algebraic expression for the scalar variance was found to be well appropriate for the modeling of small-scale mixing processes by Heinz and Roekaerts [12]. Therefore, we neglect (in consistency with the treatment of the dynamics of k_r in Section 3) all the gradients of $\bar{\phi}^2$ on the left-hand side of (4.10). This implies

$$\bar{\phi}^2 = \frac{2}{3} \ell_*^2 \frac{\tau_\varphi}{(1 - R)\tau_L} \Delta^2 \frac{\partial \bar{\Phi}}{\partial x_m} \frac{\partial \bar{\Phi}}{\partial x_m}$$

$$= \frac{2}{3} \ell_*^2 \left(1 + \frac{\tau_\varphi}{\tau_L} \right) \Delta^2 \frac{\partial \bar{\Phi}}{\partial x_m} \frac{\partial \bar{\Phi}}{\partial x_m} = \frac{2}{3} \ell_{\varphi_*}^2 \Delta^2 \frac{\partial \bar{\Phi}}{\partial x_m} \frac{\partial \bar{\Phi}}{\partial x_m}. \quad (4.12)$$

The first expression for $\overline{\phi^2}$ follows from (4.10) combined with (4.11). The second expression is obtained by calculating $R = (1 + \tau_\varphi/\tau_L)^{-1}$ according to its definition, where V_{ij} is considered to be isotropic. The last expression introduces the parameter ℓ_{φ_*} by the relation $\ell_{\varphi_*}^2 = \ell_*^2(1 + \tau_\varphi/\tau_L)$, which assures that $\overline{\phi^2}$ is calculated as a positive variable. The relation (4.12) is often used to provide the scalar SGS variance within the context of assumed-shape methods [4, 27, 42]. ℓ_{φ_*} was then calculated dynamically [42] or taken to be $\ell_{\varphi_*} = 0.5$ [4].

The definition of $\ell_{\varphi_*}^2$ can be used to obtain the following expression for the mixing frequency,

$$\frac{1}{\tau_\varphi} = \frac{\ell_*^2}{\ell_{\varphi_*}^2 - \ell_*^2} \frac{1}{\tau_L}. \quad (4.13)$$

The dependence of τ_φ^{-1} on ℓ_* corresponds to the expectation: the intensity of scalar mixing grows with the characteristic eddy length ℓ_* . ℓ_{φ_*} is a characteristic measure for the length over which the scalar field changes. The relation (4.13) provides for it the constraint $\ell_{\varphi_*} > \ell_*$. This means that the characteristic length of the scalar field has to be larger than the characteristic eddy length, which is required for the onset of scalar mixing (scalar fields that are smaller than eddies flow with them but are not dispersed). It is worth noting that the condition $\ell_{\varphi_*} > \ell_*$ is implied by the appearance of $G_{\alpha m}$ in (2.5c), which provides additional support for its consideration. (4.13) shows that the mixing frequency τ_φ^{-1} becomes smaller with growing ℓ_{φ_*} . This is the expected trend because τ_φ^{-1} has to vanish for $\ell_{\varphi_*} \gg \ell_*$. These explanations indicate that the variability of ℓ_{φ_*} is at least so high as that of ℓ_* . This is confirmed by the findings of Colucci et al. [2] and Jaber et al. [15], which reveal the need to apply different values for the constants used to parametrize τ_φ^{-1} for various flows. In addition to this, the relation (4.13) shows that the consideration of backscatter regarding τ_L also implies its consideration with regard to τ_φ .

By adopting the relation between τ_L and the dissipation time scale $\tau = k_r/\epsilon_r$ of turbulence,

$$\frac{1}{\tau_L} = \frac{1 + 1.5C_0}{2\tau}, \quad (4.14)$$

which follows from the definition of $\epsilon_r = 2k_r/[(1 + 1.5C_0)\tau_L]$, we may rewrite (4.13) into the form of the standard model for parametrizations of the scalar mixing frequency τ_φ^{-1} [33],

$$\frac{1}{\tau_\varphi} = \frac{C_\varphi}{2\tau}. \quad (4.15)$$

C_φ is a constant that is given according to (4.13) by

$$C_\varphi = (1 + 1.5C_0) \frac{\ell_*^2}{\ell_{\varphi_*}^2 - \ell_*^2}. \quad (4.16)$$

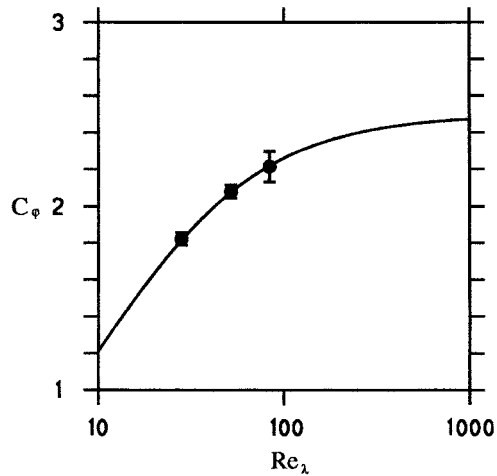


Figure 4. The calculation of C_{ϕ} in dependence on Re_{λ} according to the DNS data of Overholt and Pope [26]. The error bars denote the accuracy of these data. The solid curve gives the prediction of the parametrization (4.17) combined with $C_{\phi}(\infty) = 2.5$.

This result reveals that C_{ϕ} cannot be considered to be flow-independent because $\ell_{\phi*}$ has to be expected to vary with the scalar field considered. Thus, the consideration of scalar fields with significantly different characteristic length scales results in the need to apply different values for C_{ϕ} .

The results of DNS calculations of C_{ϕ} are given in Figure 4, which presents the findings of Overholt and Pope's [26] investigations of passive scalar mixing in homogeneous isotropic stationary turbulence with imposed constant mean scalar gradient. The data presented are the temporal average values of C_{ϕ} obtained for the stationary portion of each simulation. The C_{ϕ} value at the Taylor-scale Reynolds number $Re_{\lambda} = 185$ was not considered because it is strongly influenced by the forcing energy input [26]. The solid curve in Figure 4 represents a parametrization of the dependence of C_{ϕ} on Re_{λ} ,

$$C_{\phi} = \frac{C_{\phi}(\infty)}{1 + 1.7 C_{\phi}^2(\infty) Re_{\lambda}^{-1}}. \quad (4.17)$$

The structure of this formula is chosen according to the corresponding parametrization of C_0 suggested by Sawford [38]. Further support for such a variation of C_{ϕ} with Re_{λ} is provided by recent results of Heinz and Roekaerts [12]. The parameters in (4.17) were estimated such that the predictions of (4.17) agree with the DNS data. This leads to the asymptotic value $C_{\phi}(\infty) = 2.5$ of C_{ϕ} . The use of this value (combined with $C_0 = 19/12$ and $\ell_* = 1/3$) in (4.16) implies then $\ell_{\phi*} = 0.5$, which agrees with the assumption of Forkel and Janicka [4].

5. Summary and Further Discussion

The model (2.5a–2.5c) for the stochastic dynamics of velocities and scalars is used to improve existing LES equations for velocities and stochastic equations for the transport of scalars. The findings obtained will be summarized in Section 5.1. These investigations also enable conclusions regarding the modeling of the stochastics of SGS variables. They provide for instance insight into the variation of the parameters C_0 , ℓ_* and $\ell_{\varphi*}$ of the stochastic model (2.5a–2.5c). These results will be pointed out in Section 5.2. The difference between PDF and FDF models for turbulent flows will be summarized briefly.

5.1. THE CLOSURE OF LES EQUATIONS

The model (2.5a–2.5c) was reduced in Sections 3 and 4 to a closed LES equation for the velocity field and a scalar FDF equation (a further reduction of this FDF equation to a closed LES equation requires strong assumptions that are often not satisfied, see the detailed explanations given in Appendix C). One obtains in this way generalizations of presently applied models for the anisotropic residual stress tensor τ_{ij} and diffusion coefficient K_{ij} . Evidence for these new models is provided by the fact that they are implied by the underlying model (2.5a–2.5c), which is supported by the results of Colucci et al. [2], Jaber et al. [15], Zhou and Pereira [45] and Gicquel et al. [8]. In addition to this, the consideration of the model (2.5a–2.5c) may be seen as the analysis of a limiting case: the implications of the most simple model for the dynamics of SGS fluctuations are investigated in this way.

The algebraic models for τ_{ij} and K_{ij} presented here were compared to existing models for these quantities in Sections 3.3 and 4.2, respectively. One advantage of the new models for τ_{ij} and K_{ij} is given by their consistency. This means that different contributions to the algebraic expression (3.13) for τ_{ij} are calculated from the same model for the dynamics of instantaneous velocities, which is not the case in other methods (see Section 3.3). Further, this means that the same model for the instantaneous velocity field is used to calculate within the frame of a hybrid method the filtered velocity field and transport of scalars in physical space. This leads for instance to the theoretical estimate $Sc_t = 0.5$ for the ratio of SGS eddy viscosities for the transport of momentum and scalars, and it enables the use of the same model for the SGS stress tensor in equations for velocities and scalars (see Section 4.2). The application of such consistent methods is known to be relevant in PDF methods [24, 25, 44]. Another advantage compared to existing methods is the possibility to assess the significance of quadratic shear contributions to τ_{ij} and linear (and higher-order) shear contributions to K_{ij} . This was pointed out in Sections 3.4 and 4.2 by means of a scaling analysis. It was shown that the relevance of such contributions depends essentially on the SGS Knudsen number Kn_s , that is controlled through the numerical resolution of the flow.

5.2. THE MODELING OF THE DYNAMICS OF SGS FLUCTUATIONS

The model parameters C_0 , ℓ_* and ℓ_{φ^*} are essential ingredients of the stochastic model (2.5a–2.5c) for the dynamics of SGS fluctuations. Previously, they were estimated by means of simulations of one type of a three-dimensional flow: a temporally developing mixing layer with a Reynolds number $\text{Re} = 50\text{--}400$ [2, 8, 15]. Here, the variation of C_0 , ℓ_* and ℓ_{φ^*} was calculated analytically. For C_0 , the theoretical value $C_0 = 19/12 \approx 1.58$ was derived. This value agrees very well with the results of C_0 calculations by DNS data (see Section 3.6). It implies a value $C_K = C_0 = 19/12$ for the universal Kolmogorov constant that determines the energy spectrum (see Section 3.5). The latter result is in accord with the result $C_K = 1.62 \pm 0.17$ of measurements [40]. It is worth emphasizing that the derivation of this theoretical value for C_0 simplifies the task to adjust the model parameters to a flow considered. It enables self-consistent flow simulations through adopting the dynamic procedure (A.1) for the estimation of ℓ_* and a corresponding calculation of ℓ_{φ^*} . An alternative to this approach is to use a mean value for ℓ_* [8], which corresponds to the application of a constant c_S in LES. The estimation of such a value led to $\ell_* = 1/3 \pm 50\%$. It was shown that the mean $\ell_* = 1/3$ agrees very well with the results of DNS (see Section 3.6). The consideration of ℓ_{φ^*} led to the estimate $\ell_{\varphi^*} = 1/2$. Nevertheless, significant variations of this value (by more than 50%) have to be expected in dependence on the scalar field considered, see Section 4.3.

The results reported here do not give any hint for the need to extend (2.5a–2.5c) with terms involving interactions between the dynamics of different velocity components. As shown above, the model (2.5a–2.5c) implies models for the SGS stress tensor and diffusion coefficient that are more complex than presently applied standard models. In addition to this, the consideration of an anisotropic expression for the frequency of the velocity relaxation instead of τ_L^{-1} implies the need to introduce additional model parameters. This complicates the task to find optimal values. Thus, the structure of FDF equations is found to be much simpler than that of PDF equations for nonequilibrium flows [13]. On the other hand, the dynamic calculation of the relaxation frequencies τ_L^{-1} and τ_φ^{-1} in (2.5b–2.5c) (via dynamic procedures for the calculation of ℓ_* and ℓ_{φ^*}) corresponds to a significant modification of the simple (generation-relaxation) mechanism used previously for stochastic modeling, see the explanations given in Section 3.3. Nevertheless, the application of such (dynamic) FDF methods without adjustable parameters enables objective assessments of relevant turbulent flows which cannot be calculated by DNS.

Appendix A: The Dynamic Calculation of ℓ_*

The formula for the calculation of ℓ_* via a dynamic procedure can be obtained by extending the corresponding calculation of c_S for the Smagorinsky model [33] to the case that τ_{ij} is given through (3.13). One obtains in this way

$$\sqrt{\ell_*^2} \ell_* = \begin{cases} \frac{c_3 + c_4}{c_1 - c_2} \leq 0 & \text{if } c_3 \leq -c_4, \\ \frac{c_3 - c_4}{c_1 + c_2} \geq 0 & \text{if } c_4 \leq c_3, \end{cases} \quad (\text{A.1})$$

where the following parameters are introduced:

$$\begin{aligned} c_1 &= \frac{\kappa^2}{16\lambda^2} A_{ij} A_{ji} + B_{ij} B_{ji}, & c_2 &= \frac{\kappa}{2\lambda} A_{ij} B_{ji}, \\ c_3 &= \frac{\kappa}{4\lambda} L_{ij} A_{ji}, & c_4 &= L_{ij} B_{ji}, \end{aligned} \quad (\text{A.2})$$

The matrices in these expressions are defined through

$$\begin{aligned} L_{ij} &= \widetilde{\widetilde{U_i U_j}} - \widetilde{\widetilde{U_i}} \widetilde{\widetilde{U_j}} - \frac{1}{3} (\widetilde{\widetilde{U_n U_n}} - \widetilde{\widetilde{U_n}} \widetilde{\widetilde{U_n}}) \delta_{ij}, \\ A_{ij} &= 2\bar{\Delta}^2 |\widetilde{\widetilde{S}}| \widetilde{\widetilde{S}}_{ij} - 2\bar{\Delta}^2 |\widetilde{\widetilde{S}}|^2 \widetilde{\widetilde{S}}_{ij}, \\ B_{ij} &= \frac{\bar{\Delta}^2}{3} \left\{ 2\widetilde{\widetilde{S}}_{ik} \widetilde{\widetilde{S}}_{kj} - \frac{2}{3} \widetilde{\widetilde{S}}_{nk} \widetilde{\widetilde{S}}_{kn} \delta_{ij} - \widetilde{\widetilde{S}}_{ik} \widetilde{\widetilde{\Sigma}}_{kj} + \widetilde{\widetilde{\Sigma}}_{ik} \widetilde{\widetilde{S}}_{kj} \right\} \\ &\quad - \frac{\bar{\Delta}^2}{3} \left\{ 2\widetilde{\widetilde{S}}_{ik} \widetilde{\widetilde{S}}_{kj} - \frac{2}{3} \widetilde{\widetilde{S}}_{nk} \widetilde{\widetilde{S}}_{kn} \delta_{ij} - \widetilde{\widetilde{S}}_{ik} \widetilde{\widetilde{\Sigma}}_{kj} + \widetilde{\widetilde{\Sigma}}_{ik} \widetilde{\widetilde{S}}_{kj} \right\}. \end{aligned} \quad (\text{A.3})$$

The tilde refers to the double-filtering operation, and $\bar{\Delta}$ (which is used instead of Δ in Sections 3 and 4) and $\bar{\bar{\Delta}}$ refer to the grid and test filter width, respectively [33]. κ and λ are defined in Section 3.3. One may prove that (A.1) provides a unique determination of ℓ_* for all realizable cases. c_4 has to be positive and the case $-c_4 \leq c_3 \leq c_4$ is unrealizable.

The neglect of shear contributions of second-order (which corresponds to the assumption that τ_{ij} is given by the Smagorinsky model (3.9) instead of (3.13)) recovers the known formula for the dynamic calculation of the Smagorinsky constant c_s ,

$$\sqrt{\frac{1 + 1.5C_0}{54}} \sqrt{\ell_*^2} \ell_* = c_s = \frac{L_{ij} A_{ji}}{A_{mn} A_{nm}}. \quad (\text{A.4})$$

Appendix B: The Scalar-Conditioned Convective Flux

The velocity-scalar FDF transport equation (2.9) can be used to calculate the scalar-conditioned convective flux. One obtains (without adopting any further assumption)

$$\overline{u_i | \theta} F_\varphi = D''_{i,(1)} F_\varphi + D''_{i,(2)} F_\varphi - K_{ik} \frac{\partial F_\varphi}{\partial x_k}. \quad (\text{B.1})$$

$K_{ij} = \tau_L \gamma^{-1} \overline{u_n u_j}$ is a diffusion coefficient, where γ^{-1} refers to the inverse matrix of γ which has elements $\gamma_{ij} = \delta_{ij} + \tau_L \partial \bar{U}_i / \partial x_j$. The coefficients of the first two terms on the right-hand side of (B.1), $D''_{i,(1)}$ and $D''_{i,(2)}$ represent fluctuating drift terms that vanish in the mean. They are given by

$$D''_{i,(1)} = -\tau_L \gamma^{-1} \overline{u_m} \frac{1}{F_\varphi} \left[\frac{\partial}{\partial t} \overline{u_m | \boldsymbol{\theta}} F_\varphi + \bar{U}_k \frac{\partial}{\partial x_k} \overline{u_m | \boldsymbol{\theta}} F_\varphi \right], \quad (\text{B.2a})$$

$$\begin{aligned} D''_{i,(2)} = & -\tau_L \gamma^{-1} \overline{u_m} \frac{1}{F_\varphi} \frac{\partial}{\partial \theta_\alpha} \left[\bar{\Omega}_\alpha - \frac{1}{\tau_\varphi} (\theta_\alpha - \bar{\Phi}_\alpha) + S_\alpha \right] \overline{u_m | \boldsymbol{\theta}} F_\varphi \\ & - \tau_L \gamma^{-1} \overline{u_m} \frac{1}{F_\varphi} \frac{\partial}{\partial \theta_\alpha} G_{\alpha k} \overline{u_m u_k | \boldsymbol{\theta}} F_\varphi \\ & + \tau_L \gamma^{-1} \overline{u_m} \frac{1}{\langle \rho \rangle F_\varphi} \frac{\partial}{\partial x_j} \langle \rho \rangle (\overline{u_m u_j} - \overline{u_m u_j | \boldsymbol{\theta}}) F_\varphi. \end{aligned} \quad (\text{B.2b})$$

Contributions due to $D''_{i,(1)}$ can be neglected in accord with the neglect of such terms in the transport equation for the SGS stress tensor, see Section 3.2. To see the effects of $D''_{i,(2)}$, we consider it (in consistency with the scalar equation (2.5c)) as a linear function of scalar fluctuations,

$$D''_{i,(2)} = \tau_L \gamma^{-1} \overline{u_m} \left[\overline{S''_\alpha u_m} - \langle \rho \rangle^{-1} \frac{\partial \langle \rho \rangle \overline{u_m u_k \phi_\nu}}{\partial x_k} \right] V^{-1}_{\nu\mu} (\theta_\mu - \bar{\Phi}_\mu). \quad (\text{B.3})$$

$V^{-1}_{\nu\mu}$ refers to the inverse matrix of V which has elements $V_{\alpha\beta} = \overline{\phi_\alpha \phi_\beta}$. Expression (B.3) assures that the effect of $D''_{i,(2)}$ on the SGS scalar flux, which is given according to (B.1) by

$$\overline{u_i \phi_\alpha} = \overline{D''_{i,(1)} \phi_\alpha} + \overline{D''_{i,(2)} \phi_\alpha} - K_{ik} \frac{\partial \bar{\Phi}_\alpha}{\partial x_k}, \quad (\text{B.4})$$

is the same as that obtained by applying (B.2b) in (B.4). The first term inside the bracket of (B.3) may arise from chemical reactions. According to (B.4), its contribution to the SGS scalar flux $\overline{u_i \phi_\alpha}$ is given by $\tau_L \gamma^{-1} \overline{u_m} \overline{S''_\alpha u_m}$. The consideration of the usual structure of S_α reveals that this term involves the dependence of $\overline{u_i \phi_\alpha}$ on the scalar fluxes of all the other species. Such cross-diffusion contributions are seen to be of negligible relevance in PDF methods so that their neglect in FDF methods appears to be well justified. The second term inside the bracket of (B.3) is related to turbulent diffusion. Such contributions are also neglected usually. Therefore, $D''_{i,(2)}$ appears to be of the same minor relevance as $D''_{i,(1)}$ under many conditions.

Appendix C: The Reduction of the Scalar FDF Equation to an Assumed-Shape FDF Method

To show the conditions for the applicability of the assumed-shape approach, we will reduce the scalar FDF transport equation (4.3) to a FDF with analytical shape. For this, it is convenient to consider (4.3) in terms of the equations for stochastic realizations,

$$\frac{d}{dt}x_i^* = \bar{U}_i + \frac{1}{\langle \rho \rangle} \frac{\partial \langle \rho \rangle K_{ij}}{\partial x_j} + (2K)^{1/2}_{ij} \frac{dW_j}{dt}, \quad (\text{C.1a})$$

$$\begin{aligned} \frac{d}{dt}\Phi_\alpha^* &= \bar{\Omega}_\alpha - \frac{1}{\tau_\varphi}(\Phi_\alpha^* - \bar{\Phi}_\alpha) + \frac{1}{\langle \rho \rangle} \frac{\partial \langle \rho \rangle G_{\alpha m} K_{mj}}{\partial x_j} \\ &+ S_\alpha + G_{\alpha m} (2K)^{1/2}_{mj} \frac{dW_j}{dt}. \end{aligned} \quad (\text{C.1b})$$

In these expressions, the square root applies to the matrix K , this means one has to use the element ij of the matrix $(2K)^{1/2}$ in (C.1a) and not the square root of matrix elements.

Next, we split the problem to calculate the statistics of Φ_α^* into the problem to calculate filtered scalars $\bar{\Phi}_\alpha$ and variances $V_{\alpha\beta} = \overline{\phi_\alpha \phi_\beta}$, and the problem to calculate the statistics of standardized variables $\hat{\Phi}_\alpha^* = V^{-1/2}_{\alpha\mu} (\Phi_\mu^* - \bar{\Phi}_\mu)$. According to (C.1b), the dynamics of the latter quantities read

$$\begin{aligned} \frac{d}{dt}\hat{\Phi}_\alpha^* &= -\frac{1}{2}V^{-1/2}_{\alpha\mu} \left(\frac{dV_{\mu\nu}}{dt} + \frac{2}{\tau_\varphi}V_{\mu\nu} \right) V^{-1/2}_{\nu\beta} \hat{\Phi}_\beta^* \\ &+ \hat{S}_\alpha'' + V^{-1/2}_{\alpha\mu} G_{\mu n} (2K)^{1/2}_{nm} \frac{dW_m}{dt}, \end{aligned} \quad (\text{C.2})$$

where $\hat{S}_\alpha'' = V^{-1/2}_{\alpha\mu} S_\mu''$ refers to the rescaled fluctuation of S_α . For it we use the assumption

$$\hat{S}_\alpha'' = -\tau_\varphi^{-1} D_{\alpha\beta}^s \hat{\Phi}_\beta^*, \quad (\text{C.3})$$

where $D_{\alpha\beta}^s = (D_{\alpha\beta} + D_{\beta\alpha})/2$ is the symmetric component of generalized Damköhler numbers that are defined through $D_{\alpha\beta} = -\tau_\varphi \overline{\hat{S}_\alpha'' \hat{\Phi}_\beta^*}$. The assumption (C.3) is fully consistent with the effect of S_α'' on the scalar variances $V_{\alpha\beta}$. This may be seen by considering the variance transport equations

$$\begin{aligned} \frac{\partial V_{\alpha\beta}}{\partial t} + \bar{U}_k \frac{\partial V_{\alpha\beta}}{\partial x_k} + \langle \rho \rangle^{-1} \frac{\partial \langle \rho \rangle \overline{u_k \phi_\alpha \phi_\beta}}{\partial x_k} + \overline{u_k \phi_\beta} \frac{\partial \bar{\Phi}_\alpha}{\partial x_k} + \overline{u_k \phi_\alpha} \frac{\partial \bar{\Phi}_\beta}{\partial x_k} \\ = -\frac{2}{\tau_\varphi} V_{\alpha\beta} + G_{\alpha m} \overline{u_m \phi_\beta} + G_{\beta m} \overline{u_m \phi_\alpha} + \overline{S_\alpha'' \phi_\beta} + \overline{S_\beta'' \phi_\alpha}, \end{aligned} \quad (\text{C.4})$$

which follow from Equation (4.3). The use of (C.3) combined with (C.4) in (C.2) then results in

$$\begin{aligned} \frac{d}{dt} \hat{\Phi}_\alpha^* &= \frac{1}{2} V^{-1/2} \alpha_\mu \left(\frac{1}{\langle \rho \rangle} \frac{\partial \langle \rho \rangle \overline{u_k \phi_\mu \phi_\beta}}{\partial x_k} + \overline{u_k \phi_\beta} \frac{\partial \bar{\Phi}_\mu}{\partial x_k} \right. \\ &\quad \left. + \overline{u_k \phi_\mu} \frac{\partial \bar{\Phi}_\beta}{\partial x_k} - G_{\mu m} \overline{u_m \phi_\beta} - G_{\beta m} \overline{u_m \phi_\mu} \right) V^{-1/2} \beta_\nu \hat{\Phi}_\nu^* \\ &\quad + V^{-1/2} \alpha_\mu G_{\mu n} (2K)^{1/2} \frac{dW_m}{dt}, \end{aligned} \quad (\text{C.5})$$

where the relation $d\bar{\Phi}_\alpha/dt = \overline{d\Phi_\alpha/dt}$ is applied. Equation (C.5) reveals that the standardized variables $\hat{\Phi}_\alpha^*$ are unchanged ($d\hat{\Phi}_\alpha^*/dt = 0$) if there is no velocity-scalar correlation. The FDF of standardized variables is then known: it is equal to the initial FDF. It is worth noting that the joint initial FDF has to be provided as the product of marginal FDFs because there is no correlation between different standardized variables, $\hat{\phi}_\alpha \hat{\phi}_\beta = \delta_{\alpha\beta}$.

The calculation of the FDF via its transport equation is reduced in this case of vanishing velocity-scalar correlations to the calculation of filtered scalars and variances. We may write Equation (4.4) as

$$\frac{\partial \bar{\Phi}_\alpha}{\partial t} + \bar{U}_k \frac{\partial \bar{\Phi}_\alpha}{\partial x_k} = \langle \rho \rangle^{-1} \frac{\partial}{\partial x_k} \langle \rho \rangle (v_{(\alpha)} \delta_{km} + K_{km}) \frac{\partial \bar{\Phi}_\alpha}{\partial x_m} + V^{1/2} \alpha_\mu \bar{\hat{S}}_\mu, \quad (\text{C.6})$$

where the $V^{1/2} \alpha_\beta$ satisfy according to (C.4)

$$\frac{\partial V^{1/2} \alpha_\beta}{\partial t} + \bar{U}_k \frac{\partial V^{1/2} \alpha_\beta}{\partial x_k} = -\frac{1}{\tau_\varphi} \{ \delta_{\alpha\mu} + D_{\alpha\mu}^s \} V^{1/2} \alpha_\mu. \quad (\text{C.7})$$

Equations (C.6) and (C.7) are closed because $\bar{\hat{S}}_\mu$ and $D_{\alpha\beta}^s$ can be obtained easily if the FDF of the standardized variables is specified. Equation (C.7) reveals that only scalar fluctuations that arise from the initial conditions enter (C.6): there is no production mechanism for fluctuations if velocity-scalar correlations vanish. The scalar fluctuations then decay according to Equation (C.7).

Acknowledgements

I am thankful to H. van Dop, R. Friedrich, F.T.M. Nieuwstadt, S.B. Pope and D. Roekaerts for support and discussions which were helpful for this work. In particular, I am very thankful to D. Roekaerts for helpful comments on a draft of this paper. A part of this work was carried out as a guest of the J.M. Burgers Center for Fluid Mechanics, Delft. I am grateful to P. Givi for providing the DNS data used to evaluate the model parameters. I would like to thank the referees for valuable suggestions for improvements.

References

1. Clark, R.A., Ferziger, J.H. and Reynolds, W.C., Evaluation of subgrid-scale models using an accurately simulated turbulent flow. *J. Fluid Mech.* **91** (1979) 1–16.
2. Colucci, P.J., Jaber, F.A., Givi, P. and Pope, S.B., Filtered density function for large eddy simulations of turbulent reactive flows. *Phys. Fluids* **10** (1998) 499–515.
3. Du, S., Sawford, B.L., Wilson, J.D. and Wilson, D.J., Estimation of the Kolmogorov constant (C_0) for the Lagrangian structure function, using a second-order Lagrangian model of grid turbulence. *Phys. Fluids* **7** (1995) 3083–3090.
4. Forkel, H. and Janicka, J., Large-eddy simulation of a turbulent hydrogen diffusion flame. *Flow, Turb. Combust.* **65** (2000) 163–175.
5. Gao, F. and O'Brien, E.E., A large-eddy simulation scheme for turbulent reacting flows. *Phys. Fluids* **A5** (1993) 1282–1284.
6. Gardiner, C.W., *Handbook of Statistical Methods*. Springer-Verlag, Berlin (1983).
7. Gatski, T.B. and Speziale, C.G., On explicit algebraic stress models for complex turbulent flows. *J. Fluid Mech.* **254** (1993) 59–78.
8. Gicquel, L.Y.M., Givi, P., Jaber, F.A. and Pope, S.B., Velocity filtered density function for large eddy simulation of turbulent flows. *Phys. Fluids* **14** (2002) 1196–1213.
9. Givi, P., Model-free simulations of turbulent reactive flows. *Prog. Energy Combust. Sci.* **15** (1989) 1–107.
10. Heinz, S., Nonlinear Lagrangian equations for turbulent motion and buoyancy in inhomogeneous flows. *Phys. Fluids* **9** (1997) 703–716.
11. Heinz, S., Time scales of stratified turbulent flows and relations between second-order closure parameters and flow numbers. *Phys. Fluids* **10** (1998) 958–973.
12. Heinz, S. and Roekaerts, D., Reynolds number effects on mixing and reaction in a turbulent pipe flow. *Chem. Engrg. Sci.* **56** (2001) 3197–3210.
13. Heinz, S., On Fokker–Planck equations for turbulent reacting flows. Part 1. Probability density function for Reynolds-averaged Navier–Stokes equations. *Flow, Turb. Combust.* **70** (2003) 115–152.
14. Heinz, S., *Statistical Mechanics of Turbulent Flows*. Springer-Verlag, Berlin (2003).
15. Jaber, F.A., Colucci, P.J., James, S., Givi, P. and Pope, S.B., Filtered mass density function for large-eddy simulation of turbulent reacting flows. *J. Fluid Mech.* **401** (1999) 85–121.
16. Kaltenbach, H.-J., Gerz, T. and Schumann, U., Large-eddy simulation of homogeneous turbulence and diffusion in stably stratified flows. *J. Fluid Mech.* **280** (1994) 1–40.
17. Kosović, B., Subgrid-scale modeling for the large-eddy simulation of high-Reynolds number boundary layers. *J. Fluid Mech.* **336** (1997) 151–182.
18. Leonard, A., Large-eddy simulation of chaotic convection and beyond. In: *35th AIAA Aerospace Sciences Meeting and Exhibit*, AIAA 97-0204, Reno, NV (1997) pp. 1–8.
19. Lilly, D.K., The representation of small-scale turbulence in numerical simulation of experiments. In: Goldstine, H.H. (ed.), *Proceedings of the IBM Scientific Computing Symposium on Environmental Sciences*, Yorktown Heights, NY (1967) pp. 195–210.
20. Liu, S., Meneveau, C. and Katz, J., On the properties of similarity subgrid-scale models as deduced from measurements in a turbulent jet. *J. Fluid Mech.* **275** (1994) 83–119.
21. Lumley, J.L., Computational modeling of turbulent flows. *Adv. Appl. Mech.* **18** (1978) 123–175.
22. Madnia, C.K. and Givi, P., Direct numerical simulation and large eddy simulation of reacting homogeneous turbulence. In: Galperin, B. and Orszag, S.A. (eds.), *Large Eddy Simulations of Complex Engineering and Geophysical Flows*. Cambridge University Press, Cambridge (1993) pp. 315–346.
23. Meneveau, C. and Katz, J., Scale-invariance and turbulence models for large-eddy simulation. *Annu. Rev. Fluid Mech.* **32** (2000) 1–32.

24. Muradoglu, M., Jenny, P., Pope, S.B. and Caughey, D.A. A consistent hybrid finite-volume/particle method for the PDF equations of turbulent reactive flows. *J. Comput. Phys.* **154** (1999) 342–371.
25. Nooren, P.A., Wouters, H.A., Peeters, T.W.J. and Roekaerts, D., Monte Carlo PDF modeling of a turbulent natural-gas diffusion flame. *Combust. Theory Modeling* **1** (1997) 79–96.
26. Overholt, M.R. and Pope, S.B., Direct numerical simulation of a passive scalar with imposed mean gradient in isotropic turbulence. *Phys. Fluids* **8** (1996) 3128–3148.
27. Pierce, C. and Moin, P., A dynamic model for subgrid-scale variance and dissipation rate of a conserved scalar. *Phys. Fluids* **10** (1998) 3041–3044.
28. Piomelli, U., Cabot, W.H., Moin, P. and Lee, S., Subgrid-scale backscatter in turbulent and transitional flows. *Phys. Fluids* **A3** (1991) 1766–1771.
29. Piomelli, U., Large-eddy simulation: Achievements and challenges. *Prog. Aerosp. Sci.* **35** (1999) 335–362.
30. Pope, S.B., A more general effective viscosity hypothesis. *J. Fluid Mech.* **72** (1975) 331–340.
31. Pope, S.B., Computations of turbulent combustions: Progress and challenges. In: *23rd Symposium (International) on Combustion*, The Combustion Institute, Pittsburgh, PA (1990) pp. 591–612.
32. Pope, S.B., Lagrangian PDF methods for turbulent flows. *Annu. Rev. Fluid Mech.* **26** (1994) 23–63.
33. Pope, S.B., *Turbulent Flows*. Cambridge University Press, Cambridge (2000).
34. Réveillon, J. and Vervisch, L., Subgrid scale turbulent micromixing: Dynamic approach. *AIAA J.* **36** (1998) 336–341.
35. Risken, H., *The Fokker–Planck Equation*. Springer-Verlag, Berlin (1984).
36. Rogers, M.M., Mansour, N.N. and Reynolds, W.C., An algebraic model for the turbulent flux of a passive scalar. *J. Fluid Mech.* **203** (1989) 77–101.
37. Sagaut, P., *Large Eddy Simulation for Incompressible Flows*. Springer-Verlag, New York (2001).
38. Sawford, B.L., Reynolds number effects in Lagrangian stochastic models of turbulent dispersion. *Phys. Fluids* **A3** (1991) 1577–1586.
39. Sawford, B.L. and Yeung, P.K., Lagrangian statistics in uniform shear flow: Direct numerical simulation and Lagrangian stochastic models. *Phys. Fluids* **13** (2001) 2627–2634.
40. Sreenivasan, K.R., On the universality of the Kolmogorov constant. *Phys. Fluids* **7** (1995) 2778–2784.
41. Vreman, B., Geurts, B. and Kuerten, H., Realizability conditions for the turbulent stress tensor in large-eddy simulation. *J. Fluid Mech.* **278** (1994) 351–362.
42. Wall, C., Boersma, B.J. and Moin, P., An evaluation of the assumed beta probability density function subgrid-scale model for large eddy simulation of nonpremixed, turbulent combustion with heat release. *Phys. Fluids* **12** (2000) 2522–2529.
43. Winkelmann, G.S., Wray, A.A. and Vasilyev, O.V., Testing of a new mixed model for LES: The Leonard model supplemented by a dynamic Smagorinsky term. In: *Proceedings of Summer Program*, Center for Turbulence Research, Stanford University and NASA Ames (1998) pp. 367–388.
44. Wouters, H.A., Nooren, P.A., Peeters, T.W.J. and Roekaerts, D., Simulation of a bluff-body stabilized diffusion flame using second-moment closure and Monte Carlo methods. In: *Proceedings Twenty-Sixth Symposium (International) on Combustion*. The Combustion Institute, Pittsburgh, PA (1996) pp. 177–185.
45. Zhou, X.Y. and Pereira, J.C.F., Large eddy simulation (2D) of a reacting plane mixing layer using filtered density function closure. *Flow, Turb. Combust.* **64** (2000) 279–300.